

Mean-velocity profile of smooth channel flow explained by a cospectral budget model with wall-blockage

Kaighin A. McColl, Gabriel G. Katul, Pierre Gentine, and Dara Entekhabi

Citation: *Physics of Fluids* **28**, 035107 (2016); doi: 10.1063/1.4943599

View online: <http://dx.doi.org/10.1063/1.4943599>

View Table of Contents: <http://scitation.aip.org/content/aip/journal/pof2/28/3?ver=pdfcov>

Published by the [AIP Publishing](#)

Articles you may be interested in

[Drag reduction effect by a wave-like wall-normal body force in a turbulent channel flow](#)

Phys. Fluids **26**, 115104 (2014); 10.1063/1.4901186

[Direct numerical simulation of drag reduction in a turbulent channel flow using spanwise traveling wave-like wall deformation](#)

Phys. Fluids **25**, 105115 (2013); 10.1063/1.4826887

[Numerical modeling of the flow structures in the channels with T-junction](#)

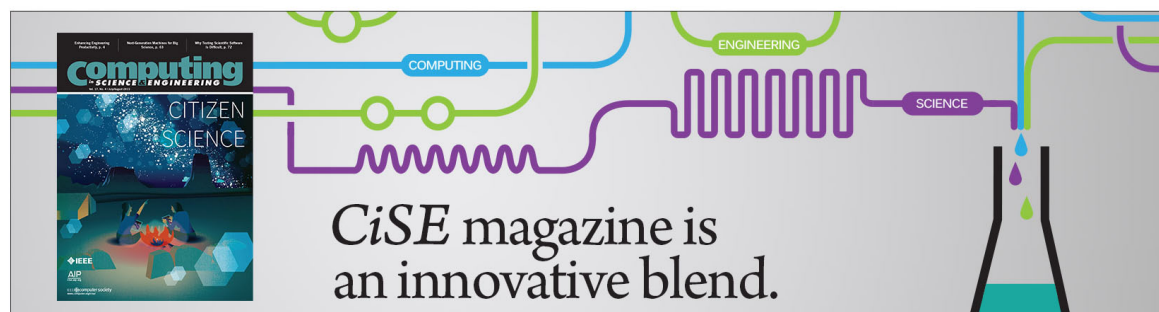
AIP Conf. Proc. **1493**, 124 (2012); 10.1063/1.4765480

[An apparent symmetry property of the mean velocity gradient in turbulent Poiseuille flows and its implications](#)

Phys. Fluids **23**, 101705 (2011); 10.1063/1.3657819

[Transient response of Reynolds stress transport to spanwise wall oscillation in a turbulent channel flow](#)

Phys. Fluids **17**, 018101 (2005); 10.1063/1.1827274

The advertisement for CiSE magazine features a stylized graphic on the left showing a network of colorful lines (blue, green, purple) connecting various nodes. Labels 'COMPUTING', 'ENGINEERING', and 'SCIENCE' are placed along these lines. Below the graphic is a small image of the magazine cover, which has 'computing SCIENCE ENGINEERING' at the top and 'CITIZEN SCIENCE' in the center. To the right of the graphic, the text 'CiSE magazine is an innovative blend.' is written in a large, black, serif font. The background is a light gray with a subtle grid pattern.

Mean-velocity profile of smooth channel flow explained by a cospectral budget model with wall-blockage

Kaighin A. McColl,^{1,a)} Gabriel G. Katul,² Pierre Gentine,³
and Dara Entekhabi^{1,4}

¹*Department of Civil and Environmental Engineering, Massachusetts Institute of Technology, Cambridge, Massachusetts 02139, USA*

²*Nicholas School of the Environment, Duke University, Durham, North Carolina 27708-0328, USA and Department of Civil and Environmental Engineering, Duke University, Durham, North Carolina 27708-0328, USA*

³*Department of Earth and Environmental Engineering, Columbia University, New York, New York 10027, USA*

⁴*Department of Earth, Atmospheric and Planetary Sciences, Massachusetts Institute of Technology, Cambridge, Massachusetts 02139, USA*

(Received 27 September 2015; accepted 28 February 2016; published online 16 March 2016)

A series of recent studies has shown that a model of the turbulent vertical velocity variance spectrum (F_{vv}) combined with a simplified cospectral budget can reproduce many macroscopic flow properties of turbulent wall-bounded flows, including various features of the mean-velocity profile (MVP), i.e., the “law of the wall”. While the approach reasonably models the MVP’s logarithmic layer, the buffer layer displays insufficient curvature compared to measurements. The assumptions are re-examined here using a direct numerical simulation (DNS) dataset at moderate Reynolds number that includes all the requisite spectral and co-spectral information. Starting with several hypotheses for the cause of the “missing” curvature in the buffer layer, it is shown that the curvature deficit is mainly due to mismatches between (i) the modelled and DNS-observed pressure-strain terms in the cospectral budget and (ii) the DNS-observed F_{vv} and the idealized form used in previous models. By replacing the current parameterization for the pressure-strain term with an expansive version that directly accounts for wall-blocking effects, the modelled and DNS reported pressure-strain profiles match each other in the buffer and logarithmic layers. Forcing the new model with DNS-reported F_{vv} rather than the idealized form previously used reproduces the missing buffer layer curvature to high fidelity thereby confirming the “spectral link” between F_{vv} and the MVP across the full profile. A broad implication of this work is that much of the macroscopic properties of the flow (such as the MVP) may be derived from the energy distribution in turbulent eddies (i.e., F_{vv}) representing the microstate of the flow, provided the link between them accounts for wall-blocking. © 2016 Author(s). All article content, except where otherwise noted, is licensed under a Creative Commons Attribution 3.0 Unported License. [<http://dx.doi.org/10.1063/1.4943599>]

I. INTRODUCTION

Wall-bounded turbulent flows are pervasive in a variety of domains, including the environment, biology, and industry. Yet even for one of the simplest, canonical cases—smooth, pressure-driven channel flow—their bulk properties have defied simplified theoretical explanation, relying predominantly on dimensional analysis or similarity arguments. One such property is the mean-velocity profile (MVP or $U(y)$), where $u = U + u'$ is the streamwise velocity, u' is the turbulent excursion, and y is the distance from the wall). von Karman¹ and Prandtl² first suggested the existence, at

^{a)} Author to whom correspondence should be addressed. Electronic mail: kmccoll@mit.edu



sufficiently high Reynolds number (Re), of a logarithmic region in the MVP away from the wall³ such that

$$U_+ = \frac{1}{\kappa} \log(y_+) + B, \quad (1)$$

where κ is the von Karman constant, B is a constant that varies with wall roughness, and the + subscript signifies normalization by wall units, i.e., the velocity and length scales u_τ and $\frac{\nu_0}{u_\tau}$, respectively, where u_τ is the friction velocity and ν_0 is the kinematic molecular viscosity. Closer to the wall, in the “viscous layer,” viscous stresses dominate turbulent stresses and U_+ is approximately linear in y_+ , with a “buffer layer” linking the linear and logarithmic regions. However, other theories, based on “incomplete similarity” reasoning for finite Reynolds number, dispute the existence of a logarithmic layer and propose its replacement with a power-law (e.g., Ref. 4).

A framework is required to explain the full MVP that moves beyond similarity arguments. Klewicki and co-authors^{5–7} have proposed an alternative, four-layer structure based on relative magnitudes of terms in the momentum budget, as observed in direct numerical simulation (DNS) and experimental data. Another potentially useful route is to consider the role of turbulent statistical fluctuations in generating macroscopic phenomena such as the MVP. L’vov *et al.*⁸ proposed a model based on the characteristic length-scales of energy-containing eddies and the Reynolds-averaged Navier Stokes equations for momentum, turbulent kinetic energy, and Reynolds stress. The variation of these length-scales over the flow profile was estimated from DNS data, resulting in a model with three parameters, independent of Reynolds number. Other studies have taken advantage of known scaling laws for turbulent fluctuations instead. Turbulent fluctuations follow Kolmogorov’s universal scaling at scales much smaller than the flow’s integral length scale, but much larger than its viscous dissipation scale.⁹ This scaling can be recovered by externally exciting the Navier-Stokes equations with a Gaussian random force with carefully chosen correlation structure. In previous studies, the dynamic renormalization group (RNG) method has been applied to obtain macroscopic flow properties from the randomly forced Navier-Stokes equations, directly linking the micro- and macro-scales of the flow.¹⁰

In a similar vein, two recent theories have proposed a “spectral link” between the MVP and the spectrum of turbulent fluctuations F , the Fourier transforms of the two-point velocity correlation functions. Gioia *et al.*¹¹ first proposed a mechanism for such a link, relying on a heuristic argument in which turbulent stresses were generated by the product of a longitudinal velocity excursion set in size by “dominant eddies” of radius y_+ , and a vertical velocity excursion determined by the turbulent kinetic energy $TKE(y_+) = \frac{1}{2} \overline{u_i^2}$, which was in turn obtained from the TKE spectrum $F_{TKE}(k)$. This phenomenological model has been shown to yield a range of known macroscopic properties of turbulent flows. These include Manning’s formula for bulk streamwise velocity in rough channel flow¹¹ and flows over submerged aquatic canopies,¹² the Reynolds number-friction factor relation in turbulent rough-impermeable pipe flow¹³ and gravel-bed (i.e., rough-permeable) flow encountered in the hyporheic zone,¹⁴ the MVP of turbulent pipe and channel flows¹¹ and the sheared, thermally stratified atmospheric surface layer (ASL),^{15,16} and the mean temperature profile of the ASL.¹⁷

An alternative mechanism is proposed by Katul and Manes¹⁸ (hereafter KM14): a simplified cospectral budget, with a parameterized pressure-strain correlation term, that links the MVP to $F_{vv}(k)$. There are two main advantages of this approach over that of Gioia *et al.*¹¹ First, it includes contributions to the turbulent stress from eddies of all sizes, not just the “dominant eddies.” Second, it links the MVP to the vertical velocity variance spectrum $F_{vv}(k)$ rather than $F_{TKE}(k)$, consistent with the production term in the turbulent stress budget. This approach has also been used to explain macroscopic relations between the turbulent Prandtl number, Monin-Obukhov stability parameter, and Richardson number in the stratified ASL.^{19–21}

The modeled MVP in KM14 matches experimental observations well in the logarithmic region (see also Ref. 22) and the viscous sublayer, where turbulent stresses are small. However, the model fails to adequately capture the strong curvature present in the buffer layer. While a number of hypotheses were proposed for the missing curvature in the buffer layer, they could not be adequately tested with the available experimental data. We use a DNS channel flow dataset at

moderate Reynolds number ($\text{Re}_\tau = \frac{u_\tau R}{\nu_0} = 2003$, where R is the channel half-width²³) to individually test several hypotheses explaining the curvature in the buffer layer, and use the outcome to propose a new model linking the spectra F_{vv} to the MVP across its full range, including the buffer layer. The new physics learned from the cospectral budget model is that the distribution of turbulent vertical velocity fluctuations (the “microstate” of the flow, represented by $F_{vv}(k)$) contains sufficient information to generate the MVP (the “macrostate” of the flow). This establishes a link between two previously unrelated areas of the turbulence literature: (1) Kolmogorov’s theory of homogeneous, isotropic turbulence, including the $k^{-5/3}$ scaling of the energy spectrum and (2) the “law of the wall” in wall-bounded turbulence. The specific value of this study is in testing and refining assumptions from previous studies by using DNS data, and making modifications to the theory where conflicts arise with the DNS data.

II. THEORY

As a starting point, the salient features of the cospectral budget model are reviewed. The once-integrated streamwise momentum budget^{3,24} is given by

$$\frac{\partial U_+}{\partial y_+} + \int_0^\infty F_{uv_+}(y_+, k_+) dk_+ = 1 - \frac{y_+}{\text{Re}_\tau}, \quad (2)$$

where $F_{uv_+}(y_+, k_+)$ is the cospectrum of the Reynolds stress at height y_+ and wavenumber k_+ . Assuming homogeneity in the spanwise direction, the Reynolds stress budget is

$$\begin{aligned} \overbrace{\frac{\partial \overline{u'v'}}{\partial t}}^{\text{Storage}} &= \overbrace{-\overline{v'^2} \frac{\partial U}{\partial y}}^{\text{Production } P_{uv}} - \overbrace{\frac{\partial \overline{u'v'v'}}{\partial y}}^{\text{Turbulent transport}} - \overbrace{\frac{1}{\bar{\rho}} \left(\frac{\partial \overline{p'v'}}{\partial x} + \frac{\partial \overline{p'u'}}{\partial y} \right)}^{\text{Pressure transport}} \\ &\quad + \underbrace{\frac{p'}{\bar{\rho}} \left(\frac{\partial u'}{\partial y} + \frac{\partial v'}{\partial x} \right)}_{\text{Pressure strain } \phi} + \underbrace{\nu_0 \left(\frac{\partial^2 \overline{u'v'}}{\partial x^2} + \frac{\partial^2 \overline{u'v'}}{\partial y^2} \right)}_{\text{Molecular diffusion}} \underbrace{-2\epsilon_{uv}}_{\text{Dissipation}}, \quad (3) \end{aligned}$$

where $\bar{\rho}$ is the mean fluid density and p' is the turbulent excursion from the mean pressure. Under stationary conditions, the storage term is ignored. Furthermore, the turbulent transport, pressure transport, and molecular diffusion terms provide relatively minor contributions, although they become more significant near the wall;³ we neglect them for now and return to this assumption later using the DNS results.

A parameterization is required for the pressure strain rate correlation ϕ that is a function of terms in the momentum and Reynolds stress budgets, to allow closure of the equations. This term is traditionally modeled as the sum of three components: slow, rapid, and wall-blocking. The slow component, generated by turbulent fluctuations, is usually modeled using Rotta’s linear return-to-isotropy form.²⁵ The rapid part, generated by the mean rate of strain, is often modeled as proportional to the production term P_{uv} .²⁶ For simplicity, the wall-blocking component was neglected in KM14 and other previous studies. Combining these components, the resulting parameterization is the Launder-Reece-Rodi Isotropization of Production (LRR-IP) model,³

$$\phi(y) = \underbrace{-C_R \frac{\overline{u'v'}(y)}{T(y)}}_{\text{Slow}} - \underbrace{C_I P_{uv}(y)}_{\text{Rapid}}, \quad (4)$$

where $C_R \approx 1.8$ is the Rotta constant that depends on the precise definition of $T(y)$, $C_I = 3/5$ is the isotropization constant predicted by Rapid Distortion Theory³ and $T(y)$ is a relaxation time scale. A spectral form of this parameterization is proposed in KM14,

$$\pi(k, y) = -C_R \text{sgn}(\overline{u'v'}) \frac{F_{uv}(k, y)}{\tau(k, y)} - C_I P_{uv}(k, y),$$

where $P_{uv}(k, y) = -F_{vv}(k, y) \frac{\partial U}{\partial y}(y)$ is a spectral form of the production term, and the relaxation time scale is $\tau(k, y) = \epsilon(y)^{-1/3} \min(k^{-2/3}, k_a(y)^{-2/3})$, where $k_a(y) = 1/y$ is a cutoff wavenumber used in

an idealized form of the F_{vv} spectrum,²⁷ described shortly. Noting that $\overline{u'v'} = \text{sgn}(\overline{u'v'}) \int_0^\infty F_{uv}(k) dk$, $\overline{v'^2} = \int_0^\infty F_{vv}(k) dk$, and $\epsilon_{uv} = \nu_0 \text{sgn}(\overline{u'v'}) \int_0^\infty k^2 F_{uv}(k) dk$, and substituting these expressions into the cospectral budget corresponding to Equation (3) yields

$$0 = -F_{vv}(k, y) \frac{\partial U}{\partial y}(y) - C_R \text{sgn}(\overline{u'v'}(y)) \frac{F_{vu}(k, y)}{\tau(k, y)} + C_I F_{vv}(k, y) \frac{\partial U}{\partial y}(y) - 2 \text{sgn}(\overline{u'v'}(y)) \nu k^2 F_{uv}(k, y). \quad (5)$$

Rearranging and nondimensionalizing to wall units yields an explicit expression for F_{uv} ,

$$F_{uv+} = -\text{sgn}(\overline{u'v'}_+) \frac{(1 - C_I) \frac{\partial U_+}{\partial y_+} F_{vv+}}{2k_+^2 + C_R \tau_+^{-1}}. \quad (6)$$

To close the system of equations, a simplified *TKE* budget is introduced, where it is assumed that *TKE* production balances dissipation,

$$\epsilon_+ = -\overline{u'v'}_+ \frac{\partial U_+}{\partial y_+} = -\frac{\partial U_+}{\partial y_+} \text{sgn}(\overline{u'v'}_+) \int_0^\infty F_{uv+}(k_+) dk_+. \quad (7)$$

This approximation is reasonable in much of the logarithmic layer, but is strongly violated closer to the wall,³ and is tested below. Combining Equations (2), (6), and (7), $\frac{\partial U_+}{\partial y_+}$ (and, therefore, the MVP) can be solved in terms of F_{vv+} .

An idealized functional form for F_{vv+} is proposed in KM14, and is shown in Fig. 1(a) (inset). This form consists of (i) the well-known $C_0 \epsilon_+^{2/3} k_+^{-5/3}$ Kolmogorov scaling⁹ in the inertial range (where C_0 is the Kolmogorov constant), (ii) a high-wavenumber dissipative range correction, (iii) a breakpoint at $k_{a+} = 1/y_+$ and transition to k_+^0 scaling, consistent with Townsend's attached-eddy hypothesis,²⁸ and (iv) a low-wavenumber correction (Fig. 1(a), inset). The bottleneck at the cross-over from inertial to viscous ranges is ignored and its effects were shown to be minor by KM14 when using the Meyers and Meneveau²⁹ formulation.

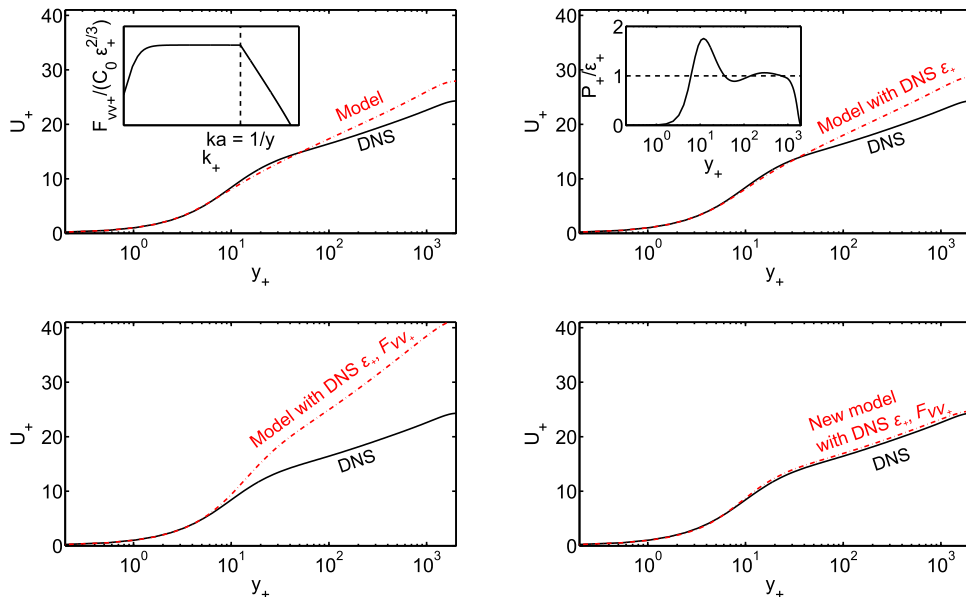


FIG. 1. Modeled (red, dotted-dashed) and DNS (black, solid) mean velocity profiles (MVPs) for four different model variants. (a) The original model used in KM14. Inset: The idealized form for the scaled vertical velocity variance spectrum F_{vv+} used in KM14, plotted on a log-log axis (solid line), where C_0 is the Kolmogorov constant and $k_{a+} = 1/y_+$ is the cutoff wavenumber (dashed line). (b) Same model as in (a), but forced with the DNS dissipation rate ϵ . Inset: Profile of the ratio between DNS TKE production P_+ and dissipation rate ϵ_+ (solid line), and the value assumed in KM14 (dashed line). (c) Same model as in (b), but forced with the DNS vertical velocity variance spectra F_{vv+} . (d) Same model as in (c), but using the new pressure-strain parameterization given in Equation (11).

III. TESTING ASSUMPTIONS WITH DNS

The missing curvature in the modeled MVP buffer layer (evident in Fig. 1(a)) may be due to the violation of one or more of the following assumptions in KM14: (1) balance between production and dissipation in the *TKE* budget, (2) the idealized shape of the F_{vv+} spectrum used, and/or (3) use of the spectral LRR-IP parameterization for the pressure-strain term in the cospectral budget. These assumptions are addressed sequentially.

A. Assumption 1: Equilibrated *TKE* budget

First, the assumption of a local balance between *TKE* production and dissipation is tested by forcing the model with DNS-reported dissipation rather than estimating it from Equation (7). The resulting profile is given in Fig. 1(b). The only discernible effect of this change is in the buffer layer, where the mean velocity is slightly increased. The reason for this change is evident from the profile of the production-to-dissipation ratio obtained from the DNS (inset of Fig. 1(b)). Around $y_+ = 12$, the production term is approximately 1.75 times the dissipation rate. However, as y_+ increases, the imbalance quickly fades to tolerably small values. Therefore, while this assumption introduces a small bias in the buffer layer, it quickly fades and does not play a significant role in the missing curvature. A possible explanation for the lack of sensitivity of the MVP to the imbalance between production and dissipation in *TKE* is due to F_{uv+} scaling as $\epsilon_+^{1/3}$, a sub-unity exponent.

B. Assumption 2: Idealized form of F_{vv+}

Second, in addition to forcing the cospectral budget model with the DNS dissipation rate, we test the effect of the assumed idealized form of the F_{vv+} spectra by forcing the model with the DNS-reported F_{vv+} spectra. We approximate the three-dimensional F_{vv+} spectra with their streamwise one-dimensional equivalents F_{vvx+} , effectively assuming isotropy. The resulting profile (Fig. 1(c)) overestimates the DNS-observed MVP. Directly comparing the DNS spectra with the idealized spectra (Fig. 2) reveals that the idealized form consistently overestimates F_{vv+} for most

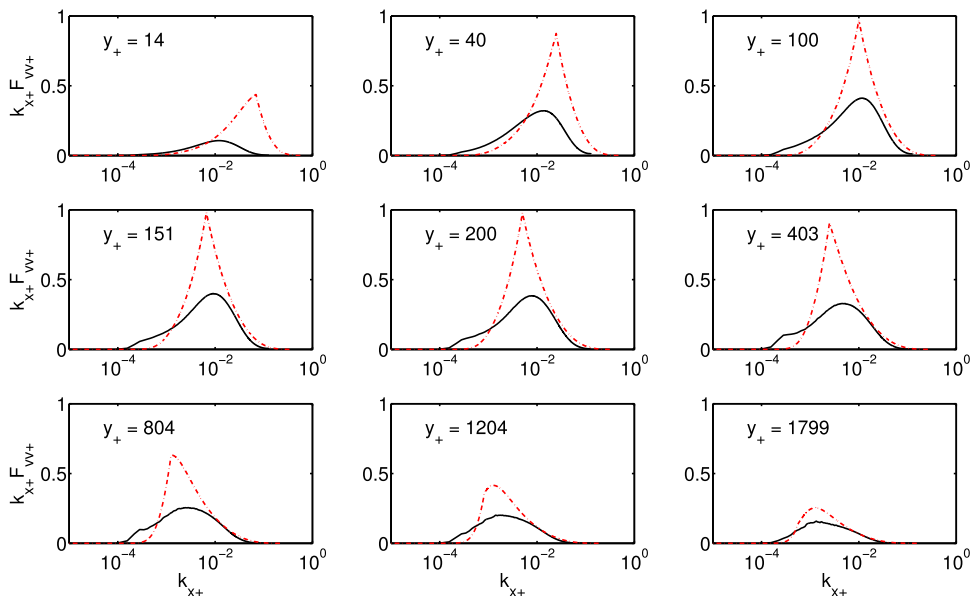


FIG. 2. Modeled (red, dotted-dashed) and DNS (black, solid) compensated streamwise vertical velocity variance spectra $k_{x+}F_{vv+}$, plotted at nine different heights y_+ . The model is the idealized form used in KM14 and given in Fig. 1(a) (inset). The compensated spectra are plotted on log-linear axes so that the areas under the curves are directly proportional to $\int_0^\infty F_{vv+}(k_+)dk_+$. The DNS spectra have been multiplied by an arbitrary constant to ensure that $\int_0^\infty F_{vv+}(k_+, y_+)dk_+ = \overline{v'^2}(y_+)$.

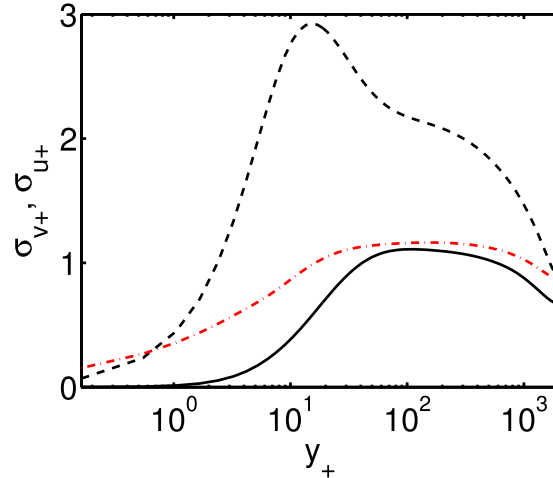


FIG. 3. Modeled (red, dotted-dashed) and DNS (black, solid) profiles of σ_{v+} (where $\sigma_{v+}^2 = \overline{v'^2}$ is the vertical velocity variance); and the DNS profile of σ_{u+} (black, dashed). The model is the variant shown in Fig. 1(b).

wavenumbers. This results in a consistently overestimated vertical velocity variance throughout the profile (Fig. 3), which was also observed in KM14 when comparing with several experiments.

Substituting Equation (6) into Equation (2) and rearranging yields

$$\frac{\partial U_+}{\partial y_+} = \frac{1 - \frac{y_+}{\text{Re}_\tau}}{1 - \text{sgn}(\overline{u'v'_+}) \int_0^\infty \frac{(1-C_I)}{2k_+^2 + C_R \tau_+^{-1}} F_{vv+} dk_+}. \quad (8)$$

It can be seen that correcting the overestimate (i.e., systematically reducing F_{vv+}) results in an increase in $\frac{\partial U_+}{\partial y_+}$ and the MVP. The mismatch between the DNS and modeled spectra is due to both the scaling and shape of the idealized form in Fig. 1(a) (inset). Inertial-range Kolmogorov scaling, as assumed in the idealized form for $k_+ > k_{a+}$, only applies when the spectral separation between y_+ and the Kolmogorov microscale is sufficiently large. Given that the DNS is at a moderate Reynolds number ($\text{Re}_\tau = 2003$), it is not surprising that the Kolmogorov inertial-range scaling tends to result in overestimated F_{vv+} . Furthermore, the DNS spectra exhibit additional regimes not captured by the current idealized form. For $y_+ < \sim 120$, the cutoff wavenumber k_{a+} appears to remain roughly constant rather than varying with height as $k_{a+} \sim \frac{1}{y_+}$ assumed in KM14. It is only for $y_+ > \sim 120$ that the cutoff wavenumber appears to begin varying with height. The invariance of k_{a+} near the wall has been noted in previous studies (e.g., Ref. 30) and is possibly the result of streaks within the buffer region that are known to not scale with distance from the wall.³¹ The four-layer model proposed by Klewicki and co-authors⁵⁻⁷ proposes a self-similar region governed by a hierarchy of length-scales linearly related to y_+ , spanning $y_+ = 2.6\sqrt{\text{Re}_\tau}$ to $y_+ = 0.5R$. For this DNS dataset, the self-similar region (and associated scaling with y_+) is predicted to begin at $y_+ = 2.6 \times \sqrt{2003} = 116$, in good agreement with the observed height at which k_{a+} begins varying with y_+ in the DNS dataset. In addition, there appear to be non-negligible contributions from a low-wavenumber mode (around $k_{x+} = 2 \times 10^{-4}$ for $y_+ > \sim 120$) in the DNS spectra that are not accounted for in the idealized form. Given the sensitivity of low-wavenumber components of calculated spectra to biases caused by smoothing and averaging, it is unclear if this is an artifact or a genuine source of variability. Since the Reynolds number of the DNS is still relatively low, we do not attempt to devise a parameterization for the DNS F_{vvx+} spectra to avoid overfitting to potentially Re-dependent features. We leave this to future studies.

C. Assumption 3: Pressure-strain parameterization

The fact that the modeled MVP degrades when forced with the DNS F_{vvx+} and dissipation rates suggests errors caused by the third assumption (the parameterization of the pressure-strain

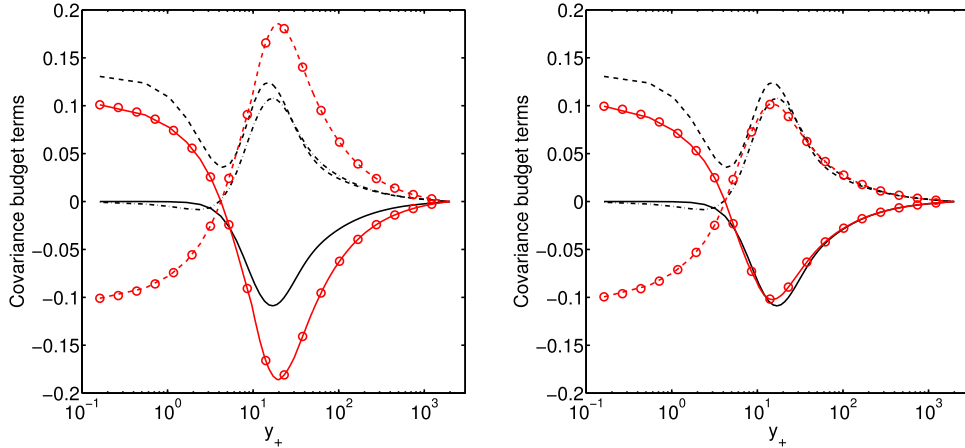


FIG. 4. Modeled (red, circle markers) and DNS (black, no markers) profiles of terms in the covariance budgets: pressure-strain (dashed), pressure-strain + neglected diffusion terms (dotted-dashed) and production (solid). Left: Using the LRR-IP pressure-strain model, generating the MVP in Fig. 1(c). Right: Using the new pressure-strain model given in Equation (11), generating the MVP in Fig. 1(d).

term) must be compensating. To test this, pressure-strain profiles from the DNS are compared to those from the LRR-IP model (Fig. 4(a)). The model significantly overestimates the DNS-reported pressure-strain profile. In the simplified cospectral budget (Equation (5)), the production term effectively balances the pressure-strain term (since the dissipation term is small). Therefore, overestimating the pressure-strain term results in a negatively biased production term. To achieve this, since F_{vv+} is prescribed, the model overestimates $\frac{\partial U_{+}}{\partial y_{+}}$ and the MVP.

IV. REVISED THEORY

Clearly, the pressure-strain correlation parameterization needs revising. The missing wall-blocking component of the pressure-strain rate correlation can be included using a standard parameterization^{26,32}

$$\phi(y) = \underbrace{-C_R \frac{\overline{u'v'}(y)}{T(y)}}_{\text{Slow}} \underbrace{-C_I P_{uv}(y)}_{\text{Rapid}} + \frac{L(y)}{y} \underbrace{\left(-C_R \frac{\overline{u'v'}(y)}{T(y)} + C_I' P_{uv}(y) \right)}_{\text{Wall-blocking}} \quad (9)$$

$$= -(C_R + C_R' \frac{L(y)}{y}) \frac{\overline{u'v'}(y)}{T(y)} - (C_I - C_I' \frac{L(y)}{y}) P_{uv}(y), \quad (10)$$

where $L(y) = TKE(y)^{3/2}/\epsilon(y)$ is a turbulent length scale. In this formulation, near the wall, the wall-blocking term increases the decorrelation effect of the slow pressure-strain component, and decreases the effect of the rapid component. A spectral version of Equation (9) may be proposed, given as

$$\pi(k, y) = -(C_R + C_R' \frac{\lambda(k, y)}{y}) \text{sgn}(\overline{u'v'}) \frac{F_{uv}(k, y)}{\tau(k, y)} - (C_I - C_I' \frac{\lambda(k, y)}{y}) P_{uv}(k, y), \quad (11)$$

where $\lambda(k, y) = \min\left(\frac{1}{k}, \frac{1}{ka(y)}\right)$ is a spectral length-scale. Choosing $C_R' = 0$ and $C_I' = 0.6$ for the new parameters, the modeled pressure-strain profile $\int_0^\infty \pi(k, y) dk$ fits the DNS pressure-strain profile reasonably outside the viscous region (Fig. 4(b)). Furthermore, it fits the sum of the DNS pressure-strain and excluded transport/diffusion terms even better, perhaps justifying the neglect of these terms in Equation (3). A desirable feature of this pressure-strain model is that, in the intermediate region ($\eta \ll k^{-1} \ll y$, where $\eta = (\nu^3/\epsilon)^{1/4}$ is the Kolmogorov microscale), $\frac{\lambda(k, y)}{y} = (ky)^{-1} \ll 1$, so

it reduces to the LRR-IP model. The LRR-IP model has been shown to generate good estimates of the inertial range cospectrum $F_{uv} = C_{uv} \frac{\partial U^+}{\partial y^+} \epsilon^{+1/3} k^{-7/3}$, including the constant $C_{uv} \approx 0.15$.^{18,22}

The resulting modeled MVP (Fig. 1(d)) fits the DNS MVP well across the entire boundary-layer depth. The fit is particularly good given that errors in estimating $\frac{\partial U^+}{\partial y^+}$ accumulate in the estimated MVP as y^+ increases. The only “tuning” that occurs is in developing the spectral pressure-strain model. Here, the parameters C'_R and C'_I are obtained by manually minimizing two objective functions: (1) the difference between $\int_0^\infty \pi(k, y) dk$ and the DNS pressure strain profile, using the DNS ϵ , F_{uv} and $\frac{\partial U}{\partial y}$ fields as inputs to Equation (11), (2) the difference between $\int_0^\infty F_{uv}(k, y) dk$ and the DNS $\overline{u'v'}$ profile, using the DNS ϵ , F_{vv} and $\frac{\partial U}{\partial y}$ fields as inputs. No tuning is performed to match the modelled MVP to the DNS MVP, further emphasizing the impact of the form of the turbulent spectrum on the MVP.

The modeled and DNS cospectra $F_{uv^+}(k_+, y_+)$ are compared in Fig. 5. While the scale of the modeled F_{uv^+} is reasonable across the profile, the shapes vary significantly. For ($y_+ > \sim 400$), the fit in the inertial range steadily improves and matches the DNS F_{uvx^+} well, consistent with other arguments.^{18,22} However, a low wavenumber mode (around $k_+ = 5 \times 10^{-4}$) dominates the DNS F_{uvx^+} cospectrum but is not present in the modeled cospectrum. The low-wavenumber mode may be an important source of missed variability. It may also be a purely numerical artifact of smoothing the estimated spectra. To further examine these different explanations, the one-dimensional streamwise and spanwise vertical velocity variance, horizontal velocity variance, and associated cospectra are shown in Figs. 6 and 7, respectively. The horizontal velocity variance spectra F_{uux^+} are greater than the corresponding vertical velocity variance spectra F_{vvx^+} across most wavenumbers, consistent with the observed profiles of horizontal and vertical velocity variance (Fig. 3). An upper bound on the cospectrum can be obtained from the Cauchy-Schwarz inequality $|F_{uv^+}(k_+)| \leq \sqrt{F_{uu^+}(k_+)F_{vv^+}(k_+)}$ (see, e.g., Ref. 33). This serves as a useful check in determining if the low wavenumber mode in the DNS F_{uvx^+} cospectrum is anomalous. As shown in Fig. 6 (bottom row), the low wavenumber mode in the compensated DNS cospectrum exceeds the upper bound given by the Cauchy-Schwarz inequality. Therefore, the low wavenumber mode appears to be an artifact of the DNS data, possibly due to the windowing and tapering process, known to particularly impact estimates of the lowest wavenumbers of the estimated (co)spectrum. This is further confirmed by examining the spanwise spectra (Fig. 7): the spanwise DNS F_{uvz^+} satisfies the Cauchy-Schwarz

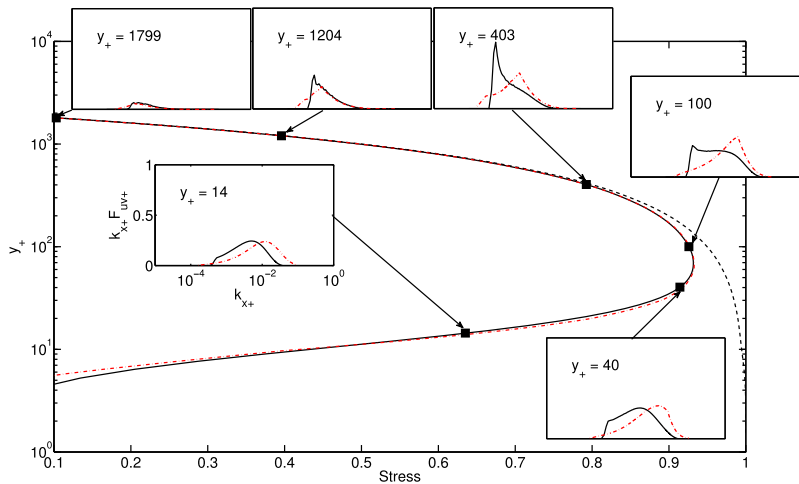


FIG. 5. Modeled (red, dotted-dashed) and DNS (black, solid) turbulent stress ($-\overline{u'v'}$) profiles, and the DNS total stress profile (black, dashed). Insets: Modeled (red, dotted-dashed) and DNS (black, solid) compensated streamwise Reynolds stress cospectra $k_{x^+} F_{uvx^+}$, plotted at six different heights y_+ (corresponding positions on the turbulent stress profile are identified with arrows and black boxes). Each inset figure has the same axis-labels as the $y_+ = 14$ inset figure, but are omitted for clarity. The modeled cospectra are obtained from the model used to generate the MVP given in Fig. 1(d). The compensated spectra are plotted on log-linear axes so that the areas under the curves are directly proportional to $\int_0^\infty F_{uvx^+}(k_+) dk_+$. The DNS cospectra have been multiplied by an arbitrary constant to ensure that $\int_0^\infty F_{uvx^+}(k_+, y_+) dk_+ = -\overline{u'v'}(y_+)$.

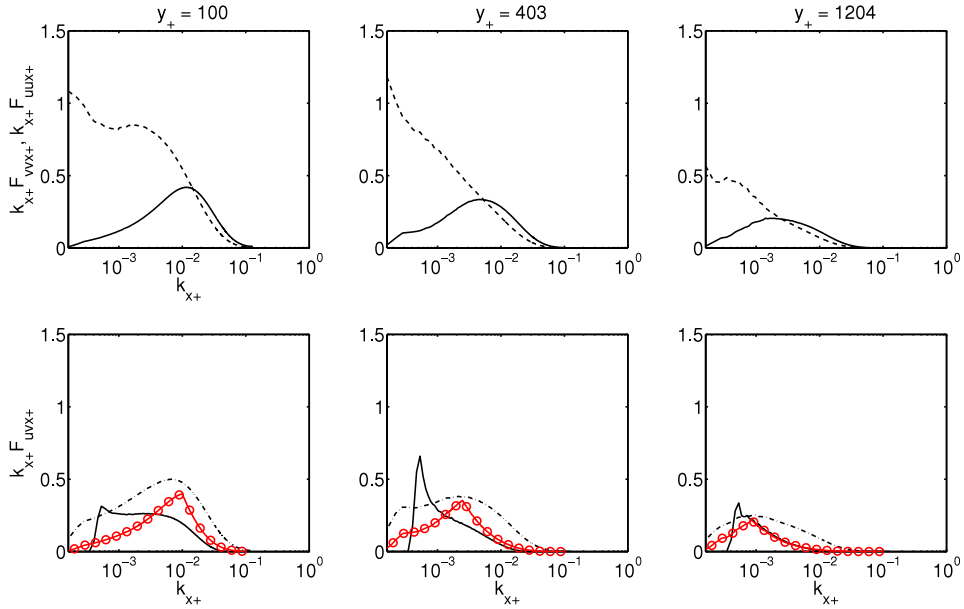


FIG. 6. Top row: Compensated streamwise horizontal velocity variance spectra $k_{x+}F_{uux+}$ (dashed lines, black) and vertical velocity variance spectra $k_{x+}F_{v vx+}$ (solid lines, black), at three different heights y_+ . Bottom row: Compensated streamwise Reynolds stress cospectra $k_{x+}F_{uvx+}$ from the DNS (solid lines, black) and model (solid lines, circle markers, red) at three different heights y_+ . A theoretical upper bound on $k_{x+}F_{uvx+}$, calculated using the Cauchy-Schwarz inequality and DNS $k_{x+}F_{uux+}$ and $k_{x+}F_{v vx+}$ is also shown (dotted-dashed lines, black). The DNS spectra and cospectra have been multiplied by an arbitrary constant to ensure that, when integrated, they give the correct DNS-observed variances and covariances, respectively.

inequality and fits the modelled cospectra reasonably well. This is expected, since low wavenumber components of the spanwise spectra are naturally dampened by the presence of side-walls in the channel and are therefore less susceptible to artifacts from smoothing and averaging. The symmetry in the spanwise direction also forces some degree of homogeneity on the flow, while the streamwise direction is highly inhomogeneous in the buffer layer due to the presence of streaks.³⁴

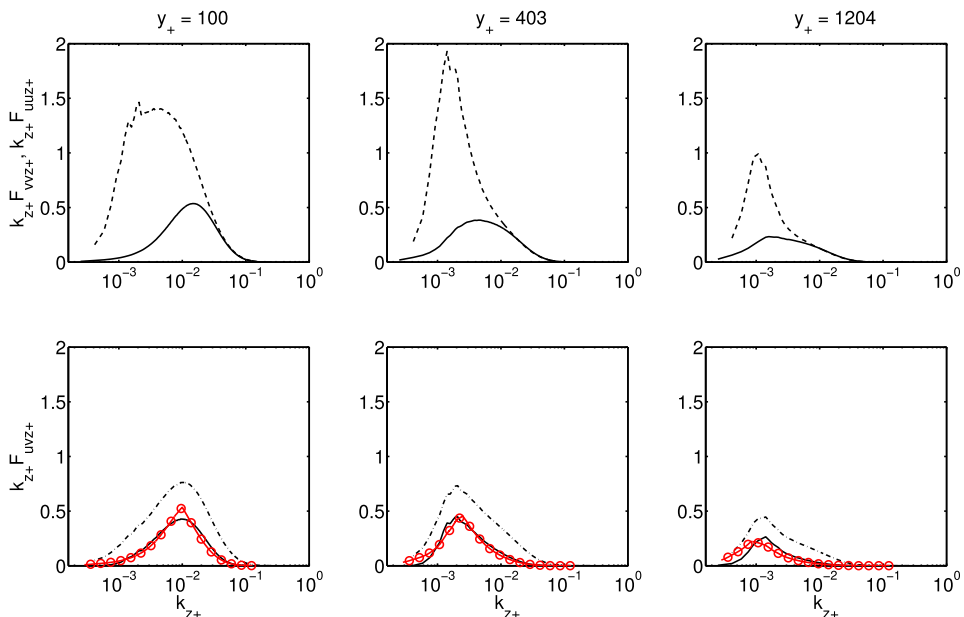


FIG. 7. Same as Fig. 6, but using spanwise (rather than streamwise) spectra and cospectra.

V. SUMMARY AND CONCLUSIONS

In summary, a cospectral budget model is shown to be capable of reproducing the full law-of-the-wall MVP with no tunable parameters, when forced with the right vertical-velocity variance spectra F_{vv+} and TKE dissipation rates. Modeling the dissipation rates by assuming a perfect balance with TKE production (and, hence, varying with $\frac{\partial U_{\pm}}{\partial y_{\pm}}$) introduces only small biases to the predicted MVP. Parameterizations used for F_{vv+} used in previous studies overestimate the true spectra, at least at the relatively low Reynolds number considered in this study. A major departure between the idealized F_{vv+} previously employed and those reported from DNS is the apparent invariance with distance from the wall, in the viscous- and lower buffer-layer, of the cross-over scale $1/k_a$ in F_{vv+} . This invariance may be due to the presence of streaks within the buffer region whose dimensions do not scale with distance from the wall.³¹ The modeled cospectra match the DNS cospectra well in their inertial ranges in regions of the flow where the turbulence is closest to fully developed. Low-wavenumber differences between modelled and DNS-observed cospectra are likely due to numerical artifacts in the DNS-observed cospectra introduced through smoothing and averaging. This study further establishes the “spectral link” between the MVP and F_{vv+} across the full boundary-layer depth. Recent studies have highlighted the significant role of very-large scale structures on near-wall turbulent stresses.^{35,36} The cospectral budget model opens up the possibility of exploring the link between these very-large scale motions (which can be parsimoniously represented by low-wavenumber peaks in the F_{vv+} spectra used as inputs to the model) and the MVP. Furthermore, relating the micro- and macro-states (i.e., the distribution of turbulent fluctuations F_{vv+} , and the MVP, respectively) through a cospectral budget may prove fruitful in explaining macroscopic properties of other wall-bounded turbulent flows, such as those subject to heating or surface roughness effects, and will be the subject of future studies.

ACKNOWLEDGMENTS

The authors thank Professor J. Jimenez, Professor R. D. Moser, Dr. J.-C. del Alamo, Dr. S. Hoyas, and Dr. P. S. Zandonade for making their DNS datasets publicly available; and two anonymous reviewers for providing critical feedback on earlier versions of this manuscript. K.A.M. is funded by the National Science Foundation’s Graduate Research Fellowship Program. G.G.K. acknowledges support from the US Department of Energy through the Office of Biological and Environmental Research Terrestrial Carbon Processes program (Nos. DE-SC0006967 and DE-SC0011461) and No. NSF-EAR-1344703. P.G. is funded by the NASA New Investigator Program NNX14AI36G, U.S. Department of Energy Early Career Award No. DE-SC0014203, and the National Science Foundation CAREER award.

¹ T. von Karman, “Mechanische Ähnlichkeit und Turbulenz,” *Nachr. Ges. Wiss. Göttingen, Math.-Phys. Kl., Fachgruppe 1* **5**, 58–76 (1930).

² L. Prandtl, “Zur turbulenten strömung in rohren und längs platten,” *Ergeb. Aerod. Versuch Göttingen* **IV**(4), 18–29 (1932).

³ S. Pope, *Turbulent Flows* (Cambridge University Press, 2000).

⁴ G. I. Barenblatt, “Scaling laws for fully developed turbulent shear flows. Part 1. Basic hypotheses and analysis,” *J. Fluid Mech.* **248**, 513–520 (1993).

⁵ T. Wei, P. Fife, J. Klewicki, and P. McMurtry, “Properties of the mean momentum balance in turbulent boundary layer, pipe and channel flows,” *J. Fluid Mech.* **522**, 303–327 (2005).

⁶ P. Fife, T. Wei, J. Klewicki, and P. McMurtry, “Stress gradient balance layers and scale hierarchies in wall-bounded turbulent flows,” *J. Fluid Mech.* **532**, 165–189 (2005).

⁷ J. C. Klewicki, “Self-similar mean dynamics in turbulent wall flows,” *J. Fluid Mech.* **718**, 596–621 (2013).

⁸ V. S. L’vov, I. Procaccia, and O. Rudenko, “Universal model of finite Reynolds number turbulent flow in channels and pipes,” *Phys. Rev. Lett.* **100**(5), 054504 (2008).

⁹ A. Kolmogorov, “The local structure of turbulence in incompressible viscous fluids for very large Reynolds numbers,” *Dokl. Akad. Nauk. SSSR* **30**, 299–303 (1941).

¹⁰ V. Yakhot and S. A. Orszag, “Renormalization group analysis of turbulence. I. Basic theory,” *J. Sci. Comput.* **1**(1), 3–51 (1986).

¹¹ G. Gioia, N. Guttenberg, N. Goldenfeld, and P. Chakraborty, “Spectral theory of the turbulent mean-velocity profile,” *Phys. Rev. Lett.* **105**(18), 184501 (2010).

¹² A. G. Konings, G. G. Katul, and S. E. Thompson, “A phenomenological model for the flow resistance over submerged vegetation,” *Water Resour. Res.* **48**(2), W02522, doi:10.1029/2011WR011000 (2012).

- ¹³ G. Gioia and P. Chakraborty, "Turbulent friction in rough pipes and the energy spectrum of the phenomenological theory," *Phys. Rev. Lett.* **96**(4), 044502 (2006).
- ¹⁴ C. Manes, L. Ridolfi, and G. Katul, "A phenomenological model to describe turbulent friction in permeable-wall flows," *Geophys. Res. Lett.* **39**(14), L14403, doi:10.1029/2012GL052369 (2012).
- ¹⁵ G. G. Katul, A. G. Konings, and A. Porporato, "Mean velocity profile in a sheared and thermally stratified atmospheric boundary layer," *Phys. Rev. Lett.* **107**(26), 268502 (2011).
- ¹⁶ S. T. Salesky, G. G. Katul, and M. Chamecki, "Buoyancy effects on the integral lengthscales and mean velocity profile in atmospheric surface layer flows," *Phys. Fluids* **25**(10), 105101 (2013).
- ¹⁷ D. Li, G. G. Katul, and E. Bou-Zeid, "Mean velocity and temperature profiles in a sheared diabatic turbulent boundary layer," *Phys. Fluids* **24**(10), 105105 (2012).
- ¹⁸ G. G. Katul and C. Manes, "Cospectral budget of turbulence explains the bulk properties of smooth pipe flow," *Phys. Rev. E* **90**(6), 063008 (2014).
- ¹⁹ G. G. Katul, A. Porporato, S. Shah, and E. Bou-Zeid, "Two phenomenological constants explain similarity laws in stably stratified turbulence," *Phys. Rev. E* **89**(2), 023007 (2014).
- ²⁰ D. Li, G. G. Katul, and S. S. Zilitinkevich, "Revisiting the turbulent Prandtl number in an idealized atmospheric surface layer," *J. Atmos. Sci.* **72**(6), 2394–2410 (2015).
- ²¹ D. Li, G. G. Katul, and E. Bou-Zeid, "Turbulent energy spectra and cospectra of momentum and heat fluxes in the stable atmospheric surface layer," *Boundary-Layer Meteorol.* **157**, 1–21 (2015).
- ²² G. G. Katul, A. Porporato, C. Manes, and C. Meneveau, "Co-spectrum and mean velocity in turbulent boundary layers," *Phys. Fluids* **25**(9), 091702 (2013).
- ²³ S. Hoyas and J. Jiménez, "Scaling of the velocity fluctuations in turbulent channels up to $Re_\tau=2003$," *Phys. Fluids* **18**(1), 011702 (2006).
- ²⁴ H. Tennekes and J. L. Lumley, *A First Course in Turbulence* (The MIT Press, Cambridge, Massachusetts, 1972).
- ²⁵ J. Rotta, "Statistische theorie nichthomogener turbulenz," *Z. Phys.* **131**(1), 51–77 (1951).
- ²⁶ B. E. Launder, G. J. Reece, and W. Rodi, "Progress in the development of a Reynolds-stress turbulence closure," *J. Fluid Mech.* **68**(03), 537–566 (1975).
- ²⁷ W. J. T. Bos, H. Touil, L. Shao, and J.-P. Bertoglio, "On the behavior of the velocity-scalar cross correlation spectrum in the inertial range," *Phys. Fluids* **16**(10), 3818–3823 (2004).
- ²⁸ A. Townsend, *The Structure of Turbulent Shear Flow* (Cambridge University Press, 1980).
- ²⁹ J. Meyers and C. Meneveau, "A functional form for the energy spectrum parametrizing bottleneck and intermittency effects," *Phys. Fluids* **20**(6), 065109 (2008).
- ³⁰ J. Jiménez, J. C. Del Álamo, and O. Flores, "The large-scale dynamics of near-wall turbulence," *J. Fluid Mech.* **505**, 179–199 (2004).
- ³¹ K. C. Kim and R. J. Adrian, "Very large-scale motion in the outer layer," *Phys. Fluids* **11**(2), 417–422 (1999).
- ³² M. M. Gibson and B. E. Launder, "Ground effects on pressure fluctuations in the atmospheric boundary layer," *J. Fluid Mech.* **86**(03), 491–511 (1978).
- ³³ P. A. O'Gorman and D. I. Pullin, "Effect of Schmidt number on the velocity-scalar cospectrum in isotropic turbulence with a mean scalar gradient," *J. Fluid Mech.* **532**, 111–140 (2005).
- ³⁴ R. Adrian, "Structure of turbulent boundary layers," in *Coherent Flow Structures at Earth's Surface* (John Wiley & Sons, 2013).
- ³⁵ I. Marusic, B. J. McKeon, P. A. Monkewitz, H. M. Nagib, A. J. Smits, and K. R. Sreenivasan, "Wall-bounded turbulent flows at high Reynolds numbers: Recent advances and key issues," *Phys. Fluids* **22**(6), 065103 (2010).
- ³⁶ M. Guala, S. E. Hommema, and R. J. Adrian, "Large-scale and very-large-scale motions in turbulent pipe flow," *J. Fluid Mech.* **554**, 521–542 (2006).